CrossMark

Photoconductivity and Luminescence Properties of Gadolinium Doped Zinc Oxide

Ravi Shankar[1] · Rajneesh Kumar Srivastava[1]

Abstract In the present work, an attempt has been made to study photoconductivity and dark conductivity in gadolinium doped zinc oxide in air as well as in vacuum synthesized by heat treatment method. Structural and morphological studies have been performed using XRD and SEM respectively. XRD indicates that ZnO:Gd (5.0%) is having mixed phase of ZnO and Gd_2O_3. SEM images of ZnO:Gd (5.0%) indicates formation of spherical shaped particles of size lying in the range of 200–400 nm. UV–visible absorption spectra in undoped ZnO and Gd doped ZnO show absorption edges at 385 and 380 nm respectively. Photoluminescence (PL) spectrum of undoped ZnO exhibits peaks centered around at 401, 418, 455, 481 and 522 nm. Gd doped ZnO exhibits almost similar peaks. The PL spectra revealed various Zn and O related native defects (eg. vacancies, interstitials, antisites etc.) Voltage dependence of photocurrent and dark current is measured at room temperature under UV–visible illumination. Rise and decay curves exhibit anomalous behavior of photocurrent in air as well as in vacuum where in the photocurrent decreases even during steady illumination.

1 Introduction

Wide-band gap II–VI semiconductors are expected to be one of the most vital materials for high-performance optoelectronics devices such as light-emitting diodes and laser diodes operating in the blue or ultraviolet spectral range. Additionally, direct gap and suitable band gap energies of these compounds makes them good candidates for high electro-optical and optoelectronic devices [1].

Zinc oxide is a wide band gap (~ 3.37 eV) and a high exciton binding energy (~ 60 meV) II–VI semiconductor material with attractive electrical and optical properties for a number of optoelectronics applications such as photonic crystals, photodetector, photodiodes, optical modulator waveguides, phosphor material in CRT screens, gas sensors, etc. [2–8].

Photoconductivity is an optical and electrical phenomenon in which a material becomes more electrically conductive due to absorption of electromagnetic radiation such as visible light, ultraviolet light or gamma radiation. Under the illumination of light, energy of the light excites the electrons from valence band to conduction band, creating additional charge carriers and thus conductivity increases. The interaction of photons having energy equal to or greater than the band gap, with bound electrons of lattice atoms, creates free electron–hole pairs [9, 10]. The photoconductivity of material depends on the carrier density and complex process of carrier generation, trapping and recombination [11]. Photoconductivity is also a function of temperature, applied field, intensity of light and energy of radiation. Rise and decay curves are governed by the trapping states and recombination centers lying inside the material and can be used to understand the nature and distribution of traps and recombination centers [12].

✉ Rajneesh Kumar Srivastava
  rkumarsau@gmail.com

[1] Department of Electronics and Communication, University of Allahabad, Allahabad 211002, India

🌀 Springer

Photoconductivity properties of a large number of materials e.g. ZnO, ZnS, CdS, CdS–Se, TiO_2, Graphene, etc. [13–22] have been studied by several researchers. Doping of semiconductors with transition metal ions and rare earth ions offer an effective approach to get tailored optical and electrical properties of semiconducting materials by introducing traps and discrete energy states in the band gap for the excited electrons. In doped compound semiconductors in contrast with the undoped ones, the impurity plays an important role in affecting the electronic energy structures and transition probabilities.

Rare earths have important characteristics in comparison to other optically active ions, the wavelengths of their emission and absorption transitions are relatively insensitive to host materials, the lifetime of metastable states are long and the quantum efficiency tends to be high. These properties lead to an excellent performance of the rare earth ions in many optical applications [23]. Many researchers have reported on photoconductivity of rare earth ions doped ZnO [24, 25]. Gd is one of the rare earth elements with atomic number 64 and a number of works have studied effect of doping of Gd on photoluminescence, electroluminescence, etc. [26–29].

In the present work, an effort, perhaps first of its kind, has been made to study the effect of doping of Gd on photoconductivity of ZnO. ZnO and Gd doped ZnO are synthesized using heat treatment method. These synthesized samples are studied for their photoconducting properties by observing voltage dependence of dark current, voltage dependence of photocurrent and rise and decay curves. Structural studies have been performed using XRD and SEM. Optical properties have been studied by UV–visible spectroscopy and photoluminescence (PL) spectroscopy.

2 Experimental Details

2.1 Chemicals

Zinc oxide (ZnO) and gadolinium oxide (Gd_2O_3) were purchased from E. Merk Ltd Mumbai. These chemicals were directly used without any special treatment.

2.2 Sample Preparation

The samples were prepared with heat treatment technique. Pure form of ZnO powder was taken and filled in ceramic tube and fired in cylindrical furnace in air. Then, it is cooled down to the room temperature and ground in a mortar to get microcrystalline form of the powder of ZnO. Sample was fired at 600 °C for 30 min. Gd doped ZnO were prepared by mixing different proportion of Gd_2O_3 into 2 gm of ZnO. The slurry was then dried in an incubator at 80 °C. The dried mixture was ground, fired and cooled down to room temperature. Figure 1 indicates that photosensitivity is maximum when doping percentage of Gd = 5.0%.

2.3 Instrumentation

The crystal structures of ZnO and ZnO:Gd were characterized by X-ray diffraction using Cu Kα radiation ($\lambda = 1.5406$ Å). The scanning electron microscopy (SEM) images were obtained using JEOL scanning electron microscope. UV–visible absorption spectrum was recorded on Perkin Elmer LS-35 spectrometer. The room temperature photoluminescence (PL) spectra of ZnO and Gd doped ZnO were obtained using Perkin Elmer LS-55 fluorescence spectrometer. In Photoconductivity study, photocurrent and dark current were measured with help of cell type device as shown in Fig. 2, which was formed by spreading a thick layer of powdered samples in between Cu electrodes etched on a Cu plate (PCB), having a space of 1 mm. The powdered layer was pressed with transparent glass plate. This glass plate has a slit for providing illumination area of 0.25 cm^2. In this cell type device, the direction of illumination is normal to the field across the electrodes. The cell was mounted in a dark chamber with a slit where from the light is allowed to fall over the cell. The UV–Vis photoresponse was measured using an Hg lamp of 300 W as a photo-excitation source. The setup used for measuring photoconductivity is shown in Fig. 3. A stabilized dc field (50–500 V/cm) was applied across the cell for the measurement of current and RISH Multi 18S with adapter RISH Multi SI 232 were connected in series. Before measuring photoconductivity of the sample, the cell is first kept in dark till it attains equilibrium. For measuring
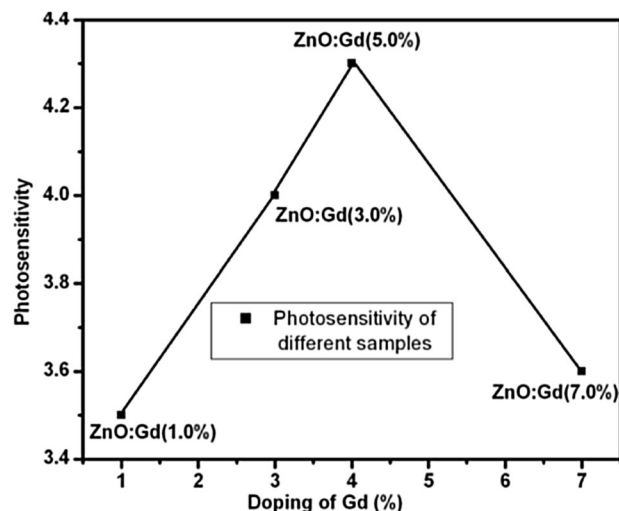

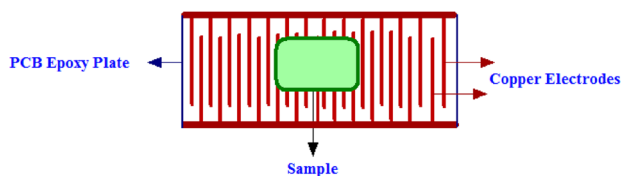
Fig. 1 Photosensitivity of prepared samples

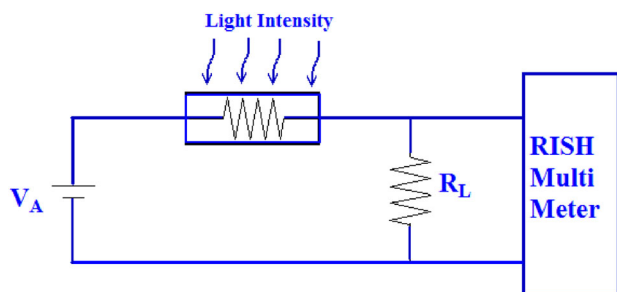**Fig. 2** Cell for photoconductivity measurement

Fig. 3 Setup for photoconductivity measurement

photoconductivity in vacuum, we used Tarson Rockyvac 300 vacuum pump to create vacuum in a glass chamber.

ZnO with concentration of gadolinium as 5.0% by weight is found to exhibit maximum photocurrent therefore ZnO and ZnO:Gd (5.0%) have been chosen for characterizations.

3 Results and Discussion

3.1 Structural Study

Figure 4 shows the XRD spectra of Gd_2O_3, ZnO and ZnO:Gd (5.0%) at room temperature synthesized by heat treatment method. The peaks at (100), (002), (101), (102) and (110) in X-ray diffraction patterns of ZnO and Gd doped ZnO indicate that ZnO is single phase with wurzite structure.

Furthermore, it can be seen that the diffraction peaks are higher and narrower, implying that ZnO is well crystallized. The XRD shows that there are additional peaks (222) and (400) of Gd_2O_3 [30, 31] in ZnO:Gd (5.0%) that establishes doping of Gd in ZnO.

3.2 Morphology Study

Figure 5 shows SEM image of ZnO:Gd (5.0%). Particles of ZnO:Gd (5.0%) is having spherical shapes. Particle size calculated from SEM images is found to lie in the range of 200–400 nm.

3.3 UV–Visible Study

The UV–visible absorption spectra of ZnO and ZnO:Gd (5.0%) are shown in Fig. 6. The occurrence of a peak shows that the absorption edge appears at 385 and 380 nm for ZnO and Gd doped ZnO respectively. The blue shift may be attributed to change in lattice structure/parameter due to doping of Gd^{3+} ions [28]. Similar UV–Vis results have been reported by Opera and Vasile, Jayachandriah et al. and Sin et al. [28, 32, 33].

3.4 Photoluminescence Study

Figure 7 shows room temperature photoluminescence (PL) spectra of ZnO and Gd doped ZnO with wavelength of excitation as 325 nm.

PL spectrum of undoped ZnO exhibits visible emission peaks: violet emission at ∼401 nm (3.08 eV) and ∼418 nm (2.96 eV), blue emission at ∼455 nm (2.71 eV), blue-green emission at ∼481 nm (2.57 eV) and green emission at ∼522 nm (2.37 eV).

The peak at ∼401 nm may be assigned to the zinc vacancy (V_{Zn}) related transition [34, 35]. Zinc interstitials (Zn_i) related emissions have been reported to be responsible for visible peak at ∼418 nm [36]. The peak at ∼455 nm may be due to singly ionized Zn interstitials (Zn_i^+) [37]. The peak at ∼481 nm has been reported as a result of transitions from the shallow donor level of zinc interstitial (Zn_i) to an acceptor level of neutral vacancy of zinc (V_{Zn}) [17, 38] whereas peak at ∼522 nm corresponds to oxygen antisites (O_{zn}) related transitions [35, 36].

Figure 7b shows PL spectrum of Gd doped ZnO wherein the peaks are almost positioned similar to those in PL spectra of ZnO but peaks at ∼ 401 and ∼ 418 nm are found to be weakened whereas the peak at ∼455 nm is found to be enhanced. There is no noticeable characteristic $4f$–$4f$ emission of doped Gd^{3+} ions. Similar results have been reported in Pr, Sm, Tb, Ho, Tm doped ZnO [37]. Absence of ZnO → Gd^{3+} transfer could be attributed to the quenching effect of defect-related emissions due to introduction of multiple impurity levels as a result of doping of Gd^{3+} ions having inappropriate energy level positions relative to VB and CB of ZnO [38–42]. Doping of Gd may be thought of reducing concentration of zinc vacancy sites and converting neutral zinc interstitials into singly ionised zinc interstitials. The schematic diagram of energy levels in PL spectra of ZnO is shown in Fig. 8.

3.5 Voltage Dependence of Dark Current

Figure 9 shows the variation of dark current (I_{dc}) with applied voltage (V) on ln–ln scale. $ln(I_{dc})$ versus $ln(V)$ curves are straight lines and can be represented by $I_{dc} \propto V^r$, where 'r' is the slope of different line segments. Both ZnO as well as Gd doped ZnO, exhibit super linear variation of dark current with applied voltage which may be attributed to injection of additional charge carriers from one of the
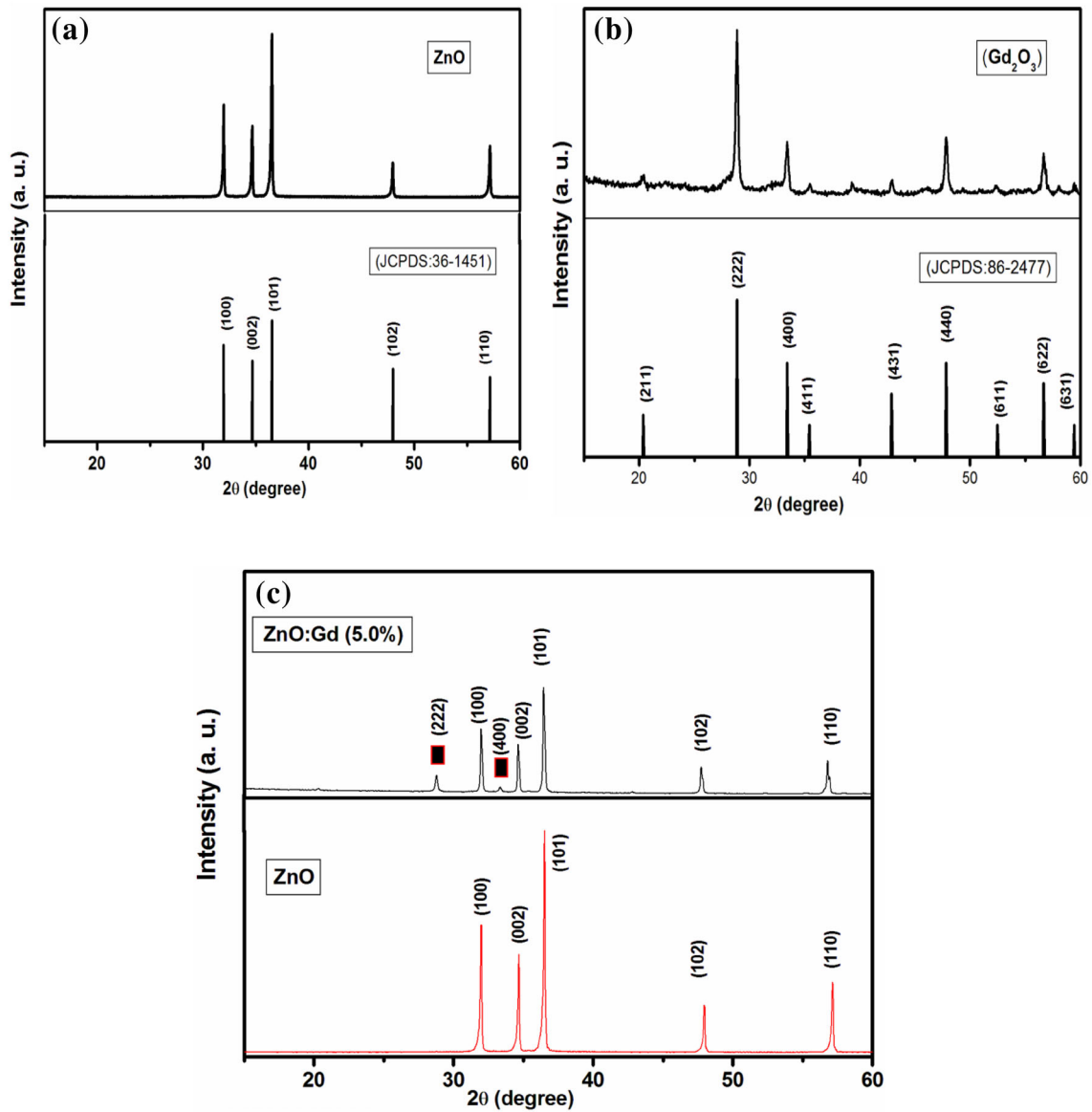
Fig. 4 **a** XRD spectra of ZnO with JCPDS. **b** XRD spectra of Gd_2O_3 with JCPDS. **c** Comparison of XRD of ZnO and Gd doped ZnO
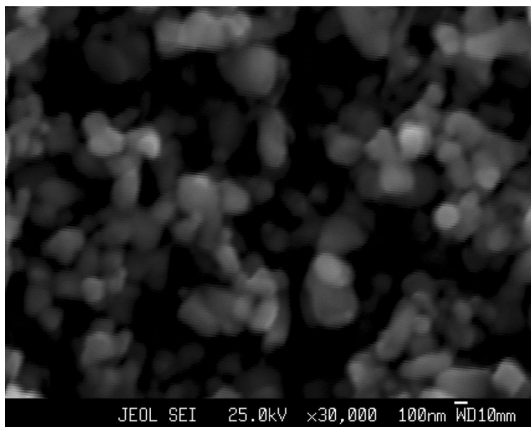

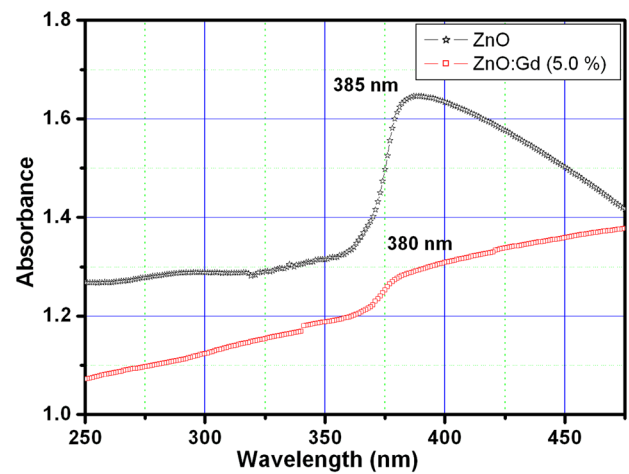
Fig. 5 SEM image of ZnO:Gd (5.0%)

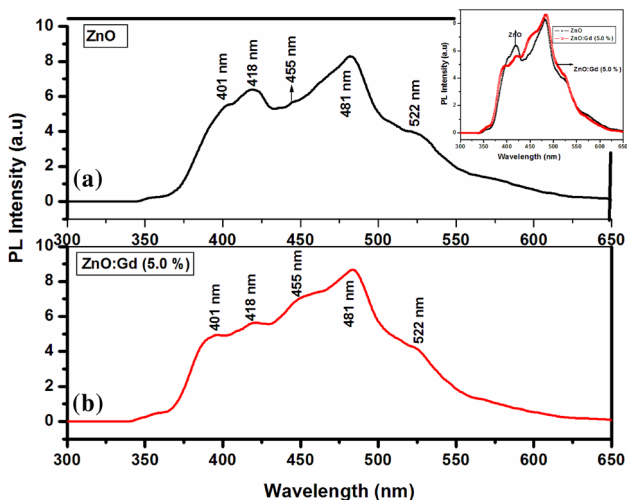**Fig. 6** UV–visible absorption spectra of ZnO and Gd doped ZnO

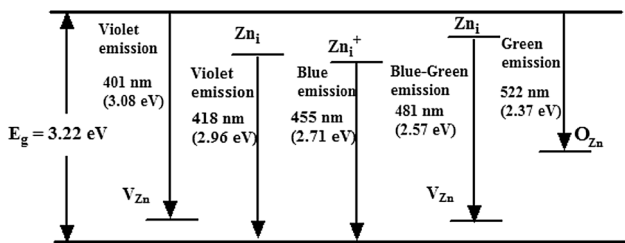Fig. 7 Photoluminescence spectra of ZnO and ZnO:Gd (5.0%)

Fig. 8 Schematic diagram of energy levels in PL spectrum of ZnO

Fig. 9 Variation of dark current with applied voltage on ln–ln scale

Fig. 10 Variation of photo current with applied voltage on ln–ln scale

electrodes [13, 43, 44]. In ZnO:Gd (5.0%), at low voltage, dark current varies with voltage according to an index greater than 2. These currents have been interpreted by Smith and Rose as space charge limited current and such type of variation was attributed to the effects of traps. Therefore, these currents may be interpreted as trap limited as well as space charge limited currents [16, 44]. There are a number of works which report ohmic nature or sublinear nature of the metal contact with a semiconductor under certain voltage and illumination conditions [2, 15, 17, 18, 22, 45–47].

3.6 Voltage Dependence of Photo Current

Figure 10 shows variation of photocurrent (I_{pc}) with applied voltage (V) on ln–ln scale. $ln(I_{pc})$ versus $ln(V)$ curves are straight lines having different slopes and can be represented by $I_{pc} \, \alpha \, V^r$, where 'r' is the slope of different line segments. At low voltage ZnO exhibits sublinear variation of photocurrent with applied voltage. Sublinear variation of photocurrent with voltage may be due to the formation of blocking contacts which do not replenish the charge carriers completely once they are captured by electrodes [13, 44]. At high voltage both the samples show super linear (r > 1) variation of photocurrent with applied
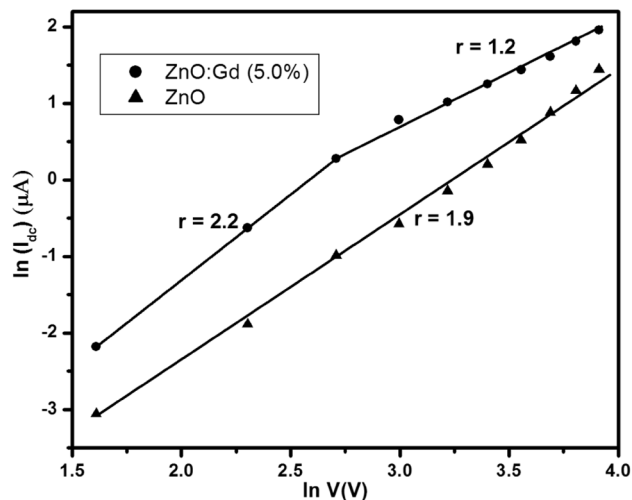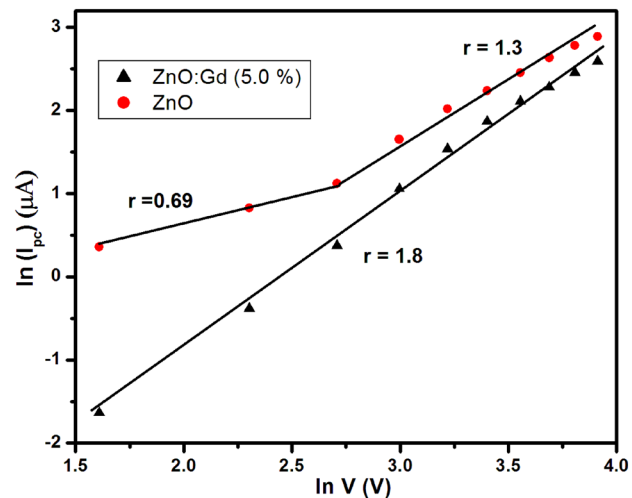
voltage due to injection of additional charge carriers from one of the electrodes [13, 16, 45–47].

3.7 Rise and Decay in Air and Vacuum

Time resolved growth and decay of photocurrent for undoped as well as gadolinium doped zinc oxide measured at room temperature in air is shown in Fig. 11. The rise and decay curves of photocurrent are governed by the trapping states and recombination centers lying in the forbidden gap of a photoconductor. Therefore these curves can be used to know about the nature and distribution of traps and recombination centers. Both the samples show fast increase in photocurrent after illumination is switched on. After attaining the peak value, the photocurrent starts decreasing even under steady illumination and eventually it stabilizes below dark current in both samples resulting in negative
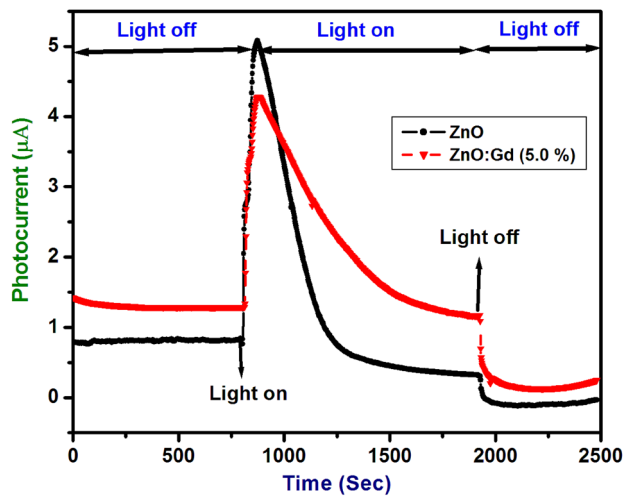
Fig. 11 Rise and decay of ZnO and ZnO: Gd (5.0%) in air

Fig. 12 Rise and decay of ZnO and ZnO: Gd (5.0%) in vacuum
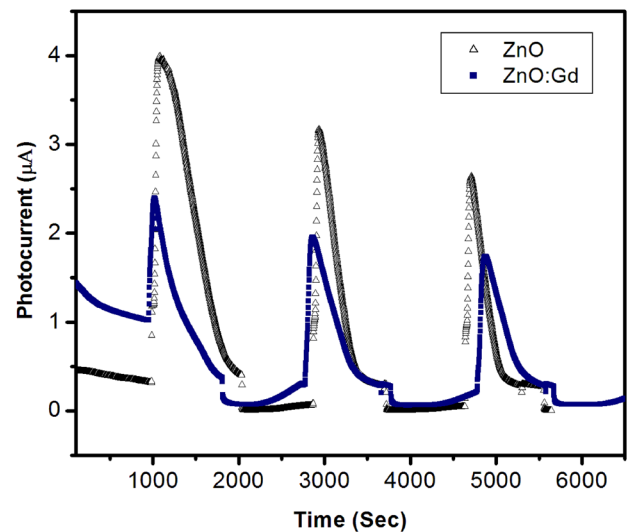
Fig. 13 Rise and decay under the periodic illumination of ZnO and Gd doped ZnO in air

photoconductivity (NPC). Negative photoconductivity is defined as the decrease of conductivity in presence of light. The negative photoconductivity is caused due to presence of imperfection centers in the forbidden gap. When illumination of the sample increases the density of the electrons or holes or both, positive photoconductivity results. With the elapse of time, if the minority carriers are also excited from the imperfection centers, negative photoconductivity results. This is due to recombination of minority carriers with majority carriers. Higher photocurrent in ZnO as compared to that in ZnO:Gd (5.0%), as shown in Table 1, may be due to lower rate of excitation of minority carriers excited from the imperfection centers with elapse of time as compared to that in ZnO:Gd (5.0%).When light is terminated the current further decreases [9, 24, 48].

Figure 12 shows the time resolved growth and decay of photocurrent for undoped as well as gadolinium doped zinc oxide measured at room temperature in vacuum. When UV–Vis light is switched on, the current increases very fast in both the samples. After attaining the peak value the photocurrent starts decreasing even under steady
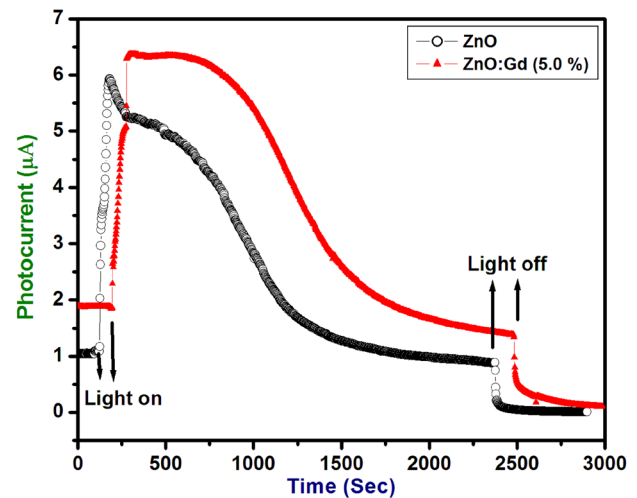
illumination. This decrease of photocurrent in vacuum is slow as compared to the decay of photocurrent in air. Similar slow decay in vacuum as compared to that in air of photocurrent has been reported by Bera and Basak [49].Í

Figure 13 shows that the results are reproducible over a number of cycles and it establishes that there is no sample degradation when illuminated with 300 W light source. During subsequent cycles peak value of photocurrent gets lowered for both the samples. Similar results have been reported by Roy et al. [50] and Bera et al. [50, 51].

4 Conclusions

In the present work, ZnO and Gd doped ZnO are synthesized by heat treatment method. Doping of Gd introduces additional peaks of Gd_2O_3 viz. (222) and (400). Particle

Table 1 Photocurrent at different applied voltages

Applied voltage (V)	Photocurrent in ZnO (μA)	Photocurrent in ZnO:Gd (5.0%) (μA)
5	1.43	0.20
10	2.29	0.68
15	3.07	1.45
20	5.21	2.88
25	7.51	4.65
30	9.37	6.45
35	11.64	8.24
40	13.94	9.78
45	16.12	11.65
50	17.98	13.37

size estimated by SEM micrographs lies in the range of 200–400 nm. In UV–Vis absorption spectra of ZnO and Gd doped ZnO, blue shifting of absorbance peak is observed. In PL spectrum of Gd doped ZnO, the peaks are almost positioned similar to those in PL spectrum of ZnO. However peaks at ∼401 and ∼418 nm in Gd doped ZnO are found to be weakened whereas the peak at ∼455 nm is found to be enhanced as compared to the corresponding peaks in undoped ZnO. Doping of Gd may be thought of reducing concentration of zinc vacancy sites and converting neutral zinc interstitials into singly ionized zinc interstitials. In undoped as well as Gd doped ZnO, dark current is found to vary super linearly with voltage. Photocurrent is found to vary sublinearly for undoped ZnO at low voltage. At high voltage, undoped ZnO as well as Gd doped ZnO, both exhibit super linear variation of photocurrent. Undoped as well as Gd doped ZnO samples are found to exhibit negative photoconductivity due to imperfection centers in forbidden gap. The rate at which the photocurrent decays in vacuum is slow as compared to that in air. No sample degradation is observed over a number of ON-OFF cycles of illumination. This is perhaps first of its kind, to study the effect of doping of Gd on photoconductivity of ZnO.

References

1. Capper P, Mauk M (2007) Liquid phase epitaxy of electronic, optical and optoelectronic materials. Wiley, London
2. Mishra SK, Srivastava RK, Prakash SG (2012) ZnO nanoparticles: structural, optical and photoconductivity characteristics. J Alloys Compd 539:1–6
3. Yadav HK, Sreenivas K, Gupta V (2010) Study of metal/ZnO based thin film ultraviolet photo detectors: the effect of induced charges on the dynamics of photoconductivity relaxation. J Appl Phys 107:044507–044509
4. Ghosh R, Fujihara S, Basak D (2006) Studies of the optoelectronic properties of ZnO thin films. J Electron Mater 35(9):1728–1733
5. Li G, Zhang J, Hou X (2014) Temperature dependence of performance of ZnO-based metal-semiconductor-metal ultraviolet photodetectors. Sens Actuat A Phys 209(1):149–153
6. Mridha S, Basak D (2006) Investigation of a p-CuO/n-ZnO thin film heterojunction for H_2 gas-sensor applications. Semicond Sci Technol 21:928–932
7. Wang ZS, Huang CH, Huang YY, Hou YJ, Xie PH et al (2001) A highly efficient solar cell made from a dye-modified ZnO-covered TiO_2 nanoporous electrode. Chem Mater 13:678–682
8. Djurisi AB, Ng AMC, Chen XY (2010) ZnO nanostructures for optoelectronics: material properties and device applications. Prog Quant Electron 34:191–259
9. Bube RH (1967) Photoconductivity of solids. Wiley, New York
10. Bube RH (1992) Photoelectronic properties of semiconductors. Cambridge University Press, New York
11. Joshi NV (1990) Photoconductivity: art: science & technology. CRC Press, NewYork
12. Rose Albert (1978) Concepts in photoconductivity and allied problems. Krieger, New York
13. Mishra SK, Srivastava RK, Prakash SG, Yadav RS, Panday AC (2010) Photoluminescence and photoconductive characteristics of hydrothermally synthesized ZnO nanoparticles. Opto Electron Rev 18(4):467–473
14. Ahn SE, Ji HJ, Kim K et al (2007) Origin of the slow photoresponse in an individual sol–gel synthesized ZnO nanowire. Appl Phys Lett 90:153106–3
15. Shankar R, Srivastava RK, Prakash SG (2013) Study of dark-conductivity and photoconductivity of ZnO nano structures synthesized by thermal decomposition of zinc oxalate. Electron Mater Lett 9(5):555–559
16. Kripal R, Gupta AK, Srivastava RK, Mishra SK (2011) Photoconductivity and photoluminescence of ZnO nanoparticles synthesized via co-precipitation method. Spectrochim Acta A 79:1605–1612
17. Mishra SK, Bayan S, Shankar R, Chakraborty P, Srivastava RK (2014) Efficient UV photosensitive and photoluminescence properties of sol–gel derived Sn doped ZnO nanostructures. Sensor Actuat A Phys 211:8–14
18. Mishra SK, Srivastava RK et al (2012) Structural, optical and photoconductivity characteristics of manganese doped cadmium sulfide nanoparticles synthesized by co-precipitation method. J Alloys Compd 513:118–124
19. Bayan S, Mishra SK, Chakraborty P, Mohanta D, Shankar R, Srivastava RK (2014) Enhanced vacuum-photoconductivity of chemically synthesized ZnO nanostructures. Philos Mag 94(9):914–924
20. Brinza M et al (2005) Photoconductivity methods in materials research. J Mater Sci Mater El 16:703–713
21. Freitag M et al (2013) Photoconductivity of biased grapheme. Nat Photonics 7:53–59
22. Srivastava RK, Pandey N, Mishra SK (2013) Effect of Cu concentration on the photoconductivity properties of ZnS nanoparticles synthesized by co-precipitation method. Mat Sci Semicon Proc 16:1659–1664
23. Shalibeik H (2007) Rare-earth-doped fiber lasers and amplifiers. Cuvillier Verlag, Germany
24. Pandey N, Srivastava RK, Prakash SG (2013) Study of dark conductivity and photoconductivity in dysprosium doped zinc oxide synthesized by heat treatment method. Natl Acad Sci Lett 36(5):521–526
25. Bhushan S, Diwan D (1986) Photoconductivity of rare earth doped ZnO. J Mater Sci Lett 5(7):723–724
26. Huang H, Ruan X et al (2007) Influence of annealing on structural, electrical and optical properties of Dy-doped ZnO thin films. J Phys D Appl Phys 40:7041–7045
27. Todkar BM, Lawangar RD, Pawar SH (1990) Electroluminescence of Gd doped Y–Ba–Cu–O superconductors. Mater Lett 9:421–424
28. Oprea O, Vasile OR et al (2012) Photoluminescence, magnetic properties and photocatalytic activity of gd^{3+} doped ZnO nanoparticles. Dig J Nanomater Bios 7(4):1757–1766
29. Ma X, Wang Z (2012) The optical properties of rare earth Gd doped ZnO nanocrystals. Mater Sci Semicond Process 15(3):227–231
30. US research nanomaterials, Gd_2O_3, XRD us-nano.com
31. Rajesh A, Raja MM, Gurunathan K (2014) Spin-relaxation of NiO encapsulated Gd_2O_3 core-Shell nanoparticles. Acta Metall Sin 27(2):253–258

32. Jayachandraiah C, Kumar SK, Krishnaiah G, Rao MN (2015) Influence of Dy dopant on structural and photoluminescence of Dy-doped ZnO nanoparticles. J Alloys Compd 623:248–254

33. Sin JC, Lam MS, Lee KT, Mohamed AR (2014) Preparation of rare earth-doped ZnO hierarchical micro/nanospheres and their enhanced photocatalytic activity under visible light irradiation. Ceram Int 40(4):5431–5440

34. Jeong SH, Kim BS, Lee BT (2003) Photoluminescence dependence of ZnO films grown on Si(100) by radio-frequency magnetron sputtering on the growth ambient. Appl Phys Lett 82:2625–2627

35. Fan XM, Lian JS, Zhao L, Liu YH (2005) Single violet luminescence emitted from ZnO films obtained by oxidation of Zn film on quartz glass. Appl Surf Sci 252(2):420–424

36. Lin B, Fu Z, Jia Y (2001) Green luminescence centres in un-doped ZnO film deposited on silicon substrate. Appl Phys Lett 79:943–945

37. Zeng X, Yuan J, Zhang L (2008) Synthesis and photoluminescent properties of rare earth Doped ZnO hierarchical microspheres. J Phys Chem C 112(10):3503–3508

38. Ma X, Wang Z (2012) The optical properties of rare earth Gd doped ZnO nanocrystals. Mat Sci Semicon Proc 15(3):227–231

39. Dorenbos P, Vanderkolk E (2006) Location of lanthanide impurity levels in the III–V semiconductor GaN. Appl Phys Lett 89:061122–061123

40. Dorenbos P, Vanderkolk E (2007) Lanthanide impurity level location in GaN, AlN, and ZnO. Proc SPIE Int Soc Opt Eng 6473:6473–153106

41. Bayan S, Mohanta D (2011) Defect mediated optical emission of randomly oriented ZnO nanorods and unusual rectifying behavior of Schottky nanojunctions. J Appl Phys 110:054316–6

42. Tatsumi T, Fujita M et al (2004) Intrinsic defects in ZnO films grown by molecular beam epitaxy. Jpn J Appl Phys 43:2602–2606

43. Devi S, Prakash SG (1994) photoconductivity studies of (PbCrO$_4$–HgO–ZnO). J Phys 43(3):245–253

44. Smith RW, Rose A (1955) Space-charge-limited currents in single crystals of cadmium sulphide. Phys Rev 97:1531–137

45. Srivastava S, Mishra SK, Yadav RS, Srivastava RK, Panday AC, Prakash SG (2010) Photoconductivity and darkconductivity studies Of Mn-Doped ZnS nanoparticles. Dig J Nanomater Bios 5(1):161–167

46. Kripal R, Gupta AK, Mishra SK, Srivastava RK, Pandey AC, Prakash SG (2010) Photoluminescence and photoconductivity of ZnS:Mn^{2+} nanoparticles synthesized via co-precipitation method. Spectrochem Acta A 76:523–530

47. Mishra SK, Srivastava RK, Prakash SG (2013) Photoluminescence and photoconductivity studies of ZnO nanoparticles prepared by solid state reaction method. J Mater Sci Mater Electron 24:125–134

48. Devi S, Prakash SG (1995) comparative study of photoconductivity in mixed lattices of PbCrO$_4$–HgO–ZnO. Int J Pure Appl Phys 33:319–322

49. Bera A, Basak D (2009) Role of defects in the anomalous photoconductivity in ZnO nanowires. Appl Phys Lett 94:163119–3

50. Roy S, Maiti DK, Panigrahi S, Basak D, Banerjee A (2014) Bolaamphiphilic amino acid appended photo-switching supramolecular gel and tuning of photo-switching behaviour. Phys Chem Chem Phys 16:6041–6049

51. Bera A, Basak D (2008) Carrier relaxation through two-electron process during photoconduction in highly UV sensitive quasi-one-dimensional ZnO nanowires. Appl Phys Lett 93:053102–053103